

Balanced Information Storage and Transfer in Modular Spiking Neural Networks

Pedro A.M. Mediano* and Murray Shanahan
Department of Computing, Imperial College London

(Dated: April 6, 2024)

While information processing in complex systems can be described in abstract, general terms, there are cases in which the relation between these computations and the physical substrate of the underlying system is itself of interest. Prominently, the brain is one such case. With the aim of relating information and dynamics in biological neural systems, we study a model network of spiking neurons with different coupling configurations, and explore the relation between its informational, dynamical, and topological properties. We find that information transfer and storage peak at two separate points for different values of the coupling parameter, and are balanced at an intermediate point. In this configuration, avalanches in the network follow a long-tailed, power law-like distribution. Furthermore, the avalanche statistics at this point reproduce empirical findings in the biological brain.

Keywords: Information processing, neural dynamics, synchronisation

I. INTRODUCTION

Information theory has been an invaluable tool for neuroscience, and in the past few decades it has been making great contributions to our understanding of neural computation and coding [11]. This has inaugurated a whole research field bringing together both disciplines [7, 16]. The broad goal of this research is to describe neural computation in abstract terms, to dissociate the cognitive process from its neural implementation. This has proven to be a fruitful and interesting endeavour, since an abstract account would allow us to compare the brain with other cognitive systems, both biological and artificial.

However, in deliberately ignoring the physical substrate of computations, a purely information-theoretic view of the brain misses some interesting research questions: what kinds of dynamical states lead to what kinds of computations? Does a particular process make use of all resources available to the neurons? Could a given computation be instantiated by a different dynamical process? To address these and other questions we must consider the specific mechanisms by which the neural physical substrate gives rise to emergent computations.

For these reasons we advocate a hybrid view of neural computation, in which information and dynamics are two sides of the same coin [5]. Along these lines, several authors have established connections between information-theoretic and dynamical properties of neural networks at several scales: specific single-neuron-level mechanisms have been found to be informationally optimal in some sense [14, 24], and on a larger scale criticality has been linked to increased information transfer [12] and information capacity [33].

In this article we continue this line of research by linking information, dynamics and topology in a modular network

of spiking neurons [32]. Specifically, we investigate the relation between dynamical criticality, aspects of information storage and transfer, and the balance between local and global coupling, matching the findings in our model with observed experimental data.

We find that information transfer and storage peak at two separate points for different values of the coupling parameter, and are balanced at an intermediate point. In this configuration, avalanches in the network follow a long-tailed, power law-like distribution. Furthermore, the avalanche statistics at this point reproduce empirical findings in the biological brain [6].

II. METHODS

We consider a system similar to the one shown in Ref. [32]. The network consists of a total of 1000 neurons, comprising one population of 200 inhibitory neurons and $n = 8$ populations (or *modules*) of 100 excitatory neurons each.

A total of 1000 internal one-directional connections (or *synapses*) are added to each excitatory module, such that any given pair of neurons are connected with probability 0.1 – resulting in modules of 10% edge density. Synapses from excitatory to inhibitory neurons are focal, with every 4 excitatory neurons in the same module projecting to the same inhibitory neuron. Every inhibitory neuron is connected to all other neurons in the network. The delay of each excitatory-excitatory synapse is sampled at random from the [1, 20]ms interval, and the delay of all other synapses is fixed at 1 ms.

Once initialised, the network is subject to a *rewiring process*, akin to the one proposed by Watts and Strogatz [37]. Watts and Strogatz’s key result is that the network undergoes a transition regime in which strong clustering coexists with short path lengths, making the network simultaneously segregated and integrated – termed a ‘small-world’ network. Here we seek to investigate how such

* pmediano@imperial.ac.uk

small-world topological properties affect the dynamical and informational behaviour of the network.

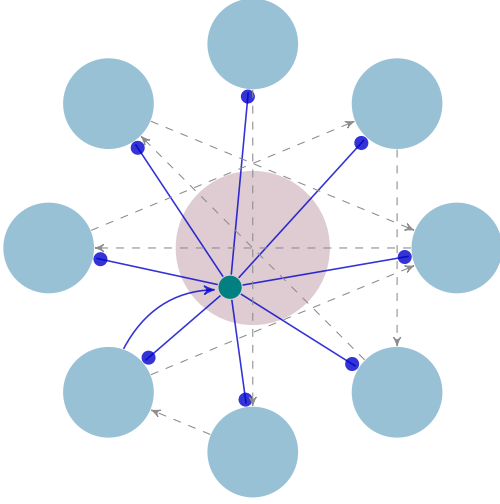


FIG. 1. Schematic diagram of the model network. There are 8 excitatory modules (light blue) connected to one another and to a larger inhibitory pool (light purple). Inhibitory neurons have diffuse connections to all the network (blue round arrows), and excitatory neurons have focal connections to inhibitory neurons (blue pointed arrow) and long-range connections between them (dashed gray arrows).

The rewiring process is only applied to the 800 excitatory neurons, and is implemented as follows. With probability p , each synapse is detached from its target neuron, and assigned a new target picked uniformly at random from any excitatory module, thus introducing inter-module synapses. This rewiring probability p effectively regulates the balance between local intra-module coupling and long-range inter-module coupling, and is the main object of analysis in this paper.

Once the topology of the network is set, we add a dynamical model to simulate the spiking behaviour of biological neurons. The dynamics of each neuron are simulated using the Izhikevich model [15],

$$\frac{dv}{dt} = 0.04v^2 + 5v + 140 - u + I \quad (1a)$$

$$\frac{du}{dt} = a(bv - u), \quad (1b)$$

where v is the membrane potential (or voltage) of the neuron, u is an auxiliary recovery variable and I is the incoming current from ingoing synapses or external sources. All quantities are in arbitrary units. When the voltage of any given neuron goes above a certain threshold we record a discrete *spike* event, such that

$$\text{if } v \geq 30, \text{ then } \begin{cases} v \leftarrow c \\ u \leftarrow u + d. \end{cases} \quad (2)$$

The values for the a, b, c, d parameters for both excitatory and inhibitory neurons are taken verbatim from Ref. [15].

We note that neurons in all populations are slightly heterogeneous, as neuron parameters are randomised.

Once the network topology and the neuron parameters are set, the network can be simulated by numerically integrating Eqs. (1) and (2). We store all the spiking events from excitatory neurons for future analysis and ignore the spikes in the inhibitory population.

A. Information Theory

Information Theory (IT) is a useful and increasingly popular tool to analyse complex systems [20, 26, 28]. We refer the reader to the classic textbook by Cover and Thomas for a general introduction to IT [10].

Throughout the paper we denote the random variable representing the activity of all excitatory neurons at time t by S_t . The system is partitioned in 8 parts, corresponding to the 8 modules of excitatory neurons described above. The time series of module i is denoted by $M_{i,t}$. We reserve the symbols X, Y, Z for arbitrary random variables.

A cornerstone of IT, Mutual Information (MI) can be used to quantify interdependence between two random time series X_t, Y_t . More precisely, it measures the reduction in uncertainty about X_t that results from observing the value of Y_t (or viceversa). One of the many ways to define mutual information is

$$\text{MI}(X_t, Y_t) = H(X_t) + H(Y_t) - H(X_t, Y_t), \quad (3)$$

where H is the standard Shannon entropy. Note that MI is a bivariate measure. To quantify how much information is shared between all $n = 8$ parts of our system we use multiinformation (also called *total information*, TI), one possible multivariate extension of MI [34]. TI is defined based on Eq. (3) as

$$\text{TI}(S_t) = \sum_{i=1}^n H(M_{i,t}) - H(S_t). \quad (4)$$

Our study adopts the framework for information processing in complex systems introduced by Lizier [18]. According to Lizier and others, distributed information processing in complex systems is the interaction between three processes: information storage, information transfer and information modification. A sound, rigorous account of information modification is still an open problem, so we will restrict our analysis to storage and transfer.

We first study information storage, following Ref. [23]. We define the entropy rate of a time series $H_\mu(X_t)$ as the entropy generated by one single timestep of the series, given all its previous history – i.e.

$$H_\mu(X_t) = \lim_{k \rightarrow \infty} H(X_t | X_{t-1}, X_{t-2}, \dots, X_{t-k}). \quad (5)$$

This quantity measures the amount of information in the time series that is fundamentally unpredictable; and enables us to write the following nonnegative decomposition of $H(X_t)$:

$$H(X_t) = \text{AIS}(X_t) + H_\mu(X_t) , \quad (6)$$

where the quantity of interest is AIS, the *active information storage*. This decomposition is intuitively interpretable: the information needed to predict step t in the time series is the information stored in its entire previous history, plus the new information being generated. In other words, AIS quantifies how much information about the history of the system is useful in predicting the system's next state. Importantly for our purposes, it has also been proposed as a tool to understand distributed computation in neural and complex systems [38]. As the $k \rightarrow \infty$ limit is (for obvious reasons) intractable, we write the finite- k approximation of the AIS of module i as

$$\text{AIS}_k(M_{i,t}) = \text{MI}(M_{i,t}^{(k)}, M_{i,t+1}) , \quad (7)$$

where $X_t^{(k)}$ is the k -dimensional embedding vector of X at time t , that contains the past k values of X up to and including time t . The aim of this embedding vector is to capture the state of the underlying dynamical process, and can be viewed as a state-space reconstruction in the Takens sense [35].

To further understand the informational properties of the network, we measure information transfer with *transfer entropy* (TE) [30]. TE quantifies to what extent knowledge of X_t contributes to predicting the future of Y_t beyond the information provided by the past of Y_t alone, and it is defined as

$$\text{TE}_k(X \rightarrow Y) = \text{MI}(X_t^{(k)}, Y_{t+1} | Y_t^{(k)}) . \quad (8)$$

There is a great body of theory behind TE as a measure of information transfer, and it is closely related to causality in the Wiener-Granger sense [4, 21]. However, when there are more variables in the system apart from X and Y , TE does not capture exactly the immediate influence of X on Y – there may be other higher-order interactions, mediated by other variables in the system [22]. For example, there could be another variable Z influencing both X and Y at different timescales, which could distort the measurement. To measure exclusively the direct transfer from X to Y without the influence of Z , we define the *conditional transfer entropy* as

$$\text{CTE}_k(X \rightarrow Y | Z) = \text{MI}(X_t^{(k)}, Y_{t+1} | Y_t^{(k)}, Z_t^{(k)}) . \quad (9)$$

Finally, we use CTE to define a nonparametric version of *causal density* (CD), slightly different from the conventional formulation [31]. We define CD as the average pairwise CTE conditioned on the rest of the system, i.e.

$$\text{CD}_k(S_t) = \frac{1}{n(n-1)} \sum_{ij} \text{CTE}_k(M_{i,t} \rightarrow M_{j,t} | S_t^{[ij]}) , \quad (10)$$

where $S_t^{[ij]}$ represents the whole system S_t with variables $M_{i,t}$ and $M_{j,t}$ removed. This formulation is equivalent to the conventional one (up to a constant) if all variables are Gaussian-distributed [3]. Within this framework, we interpret CD as a global average measure of information transfer.

From a different perspective, CD can be also thought of as quantifying dynamical complexity [36], an early branch of research in complex neural systems now embodied in Integrated Information Theory [2]. A system is said to have high dynamical complexity if it displays a balance of segregation (to the extent that its parts behave independently) and integration (to the extent that the whole system acts as one). In a completely segregated system in which the elements act independently there can be no information transfer and CD is trivially null. On the other end, in a completely integrated system in which all elements are heavily correlated, element i will provide no additional information about j beyond the information provided by the rest of the system $X^{[ij]}$, and CD is again null. Thus, CD also provides a principled measure of dynamical complexity.

III. RESULTS

We generate 400 networks with different values of p sampled uniformly at random in the $[0, 1)$ interval, and another 200 with p sampled exponentially at random in the $(10^{-2}, 1)$ interval. This is to have dense coverage of the parameter space at the low end of the range. The activity of each network is simulated using the NeMo library [13] for 200s using the RK4 method with a timestep of 0.2ms, and subsampled to a resolution of 1ms. The first 1s of simulation is discarded to avoid transient effects. Information-theoretic quantities are calculated using the implementation in [19] and are reported in bits.

A. Model Behaviour

In this section we give a qualitative summary of the behaviour of the model that will help interpretation of quantitative findings described in the rest of the paper. Spike raster plots of representative runs of the network with different values of p are shown in Fig. 2.

We begin with the fully modular network, the $p = 0$ case (bottom panel in Fig. 2). In this setting there are no direct connections between the excitatory modules. When any neurons in an excitatory module become active, the high density of intra-module synapses ensures that all neurons in the module quickly become activated.

Through the focal excitatory-inhibitory synapses, the active module feeds charge to the subset of inhibitory neurons assigned to it. These start spiking rapidly, and

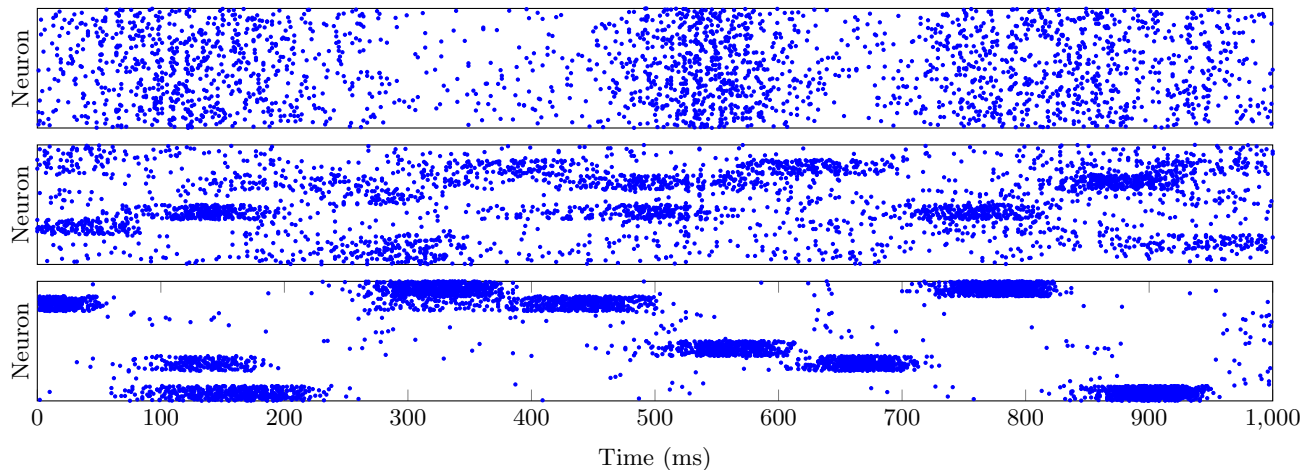


FIG. 2. Sample runs of the network for different values of the rewiring probability p . The values are $p = 0.9$ (top), 0.2 (middle) and 0 (bottom). As p increases the system transitions from multistable competitive dynamics to oscillatory cooperative dynamics.

because of the diffuse connections they shut down the activity in all other excitatory modules. This results in competitive multistable dynamics, as one module gaining control of the network prevents all others from doing so. In computational neuroscience this kind of competition mechanism is known as Winner-Take-All (WTA). Subsequently, the active module saturates and the refractory period of the neurons makes it cease firing, so that other module can take over.

At the other end of the parameter range, at $p = 0.9$ (top panel in Fig. 2), the dynamics are very different. Topologically, this setting corresponds to a fully random, Erdős-Rényi network. There is no notion of modules anymore, and all excitatory neurons are statistically equivalent. The result is an interaction between a uniform population of excitatory neurons with a smaller group of inhibitory neurons. This is reminiscent of a known mechanism of oscillation generation – a PING architecture [8]. The interplay between excitation and inhibition and the synaptic delays between them make the whole system oscillate. In this regime the modules are strongly correlated and cooperate in maintaining the global oscillation.

Finally, at intermediate values of p (middle panel in Fig. 2), these two opposite trends coexist. The dynamics of the system are more chaotic and there is no clear pattern. Local and long-range coupling are balanced and both affect the emergent dynamics (we recall that the total number of connections is fixed, so an increase in long-range coupling is always at the expense of a weaker intra-module coupling).

This transition is also interpretable as an emergent synchronisation phenomenon. For low p the WTA mechanism pushes the modules out of phase, and the network is maximally desynchronised. Conversely, for high p the modules blend together and the synchrony between them increases.

In summary, the model we described features a transition from a competitive to cooperative regime, controlled by a continuous parameter. This model naturally interpolates between two neural circuits ubiquitously present in the cortex: PING oscillators and multistable WTA circuits. As we describe below, it is between these two extremes where critical dynamics and complex information processing take place.

B. Avalanche Statistics

The seminal work of Beggs and Plenz [6] set out the search for criticality in neural systems, in particular through the analysis of avalanche statistics. A *neural avalanche* is defined as a period of continued spiking activity – i.e. a period in which the activity of a neural population is continuously above a certain *avalanche threshold*. The *avalanche size* is the total number of spikes fired by all neurons in the population between any two points of below-threshold activity.

By counting occurrences of avalanches in the network and recording their size we obtain the *avalanche size distribution*, a very relevant mathematical construct subject of much study in statistical physics and complex systems research. A common signature of critical dynamics and phase transitions is that avalanche sizes follow a *power law distribution* [29], defined as

$$P(s) \propto s^{-\alpha}, \quad (11)$$

where α is called the *critical exponent*. Beggs and Plenz's key result is that measured activity in the biological brain consistently follows a power law avalanche size distribution – leading to the hypothesis that the brain operates in a critical regime. Although their claims on criticality have

been contested [27], their empirical finding of power law distributions in neural recordings is widely accepted.

In this section we present the avalanche analysis of the resulting activity of our model. As a general methodological note, we mention that estimating and evaluating power laws when working with empirical data is remarkably complicated. In this analysis we use the methods and implementation provided in [1, 9].

We generate and run networks for many values of p as described above and measure avalanches in each module. To do this we calculate the mean firing rate of each module over 1 ms bins and run the analysis with an avalanche threshold of 3 spikes/ms. The distributions of the 8 modules in the same run of the experiment are aggregated together to improve statistics. Log-log avalanche size histograms are shown for evenly spaced values of p in Fig. 3.

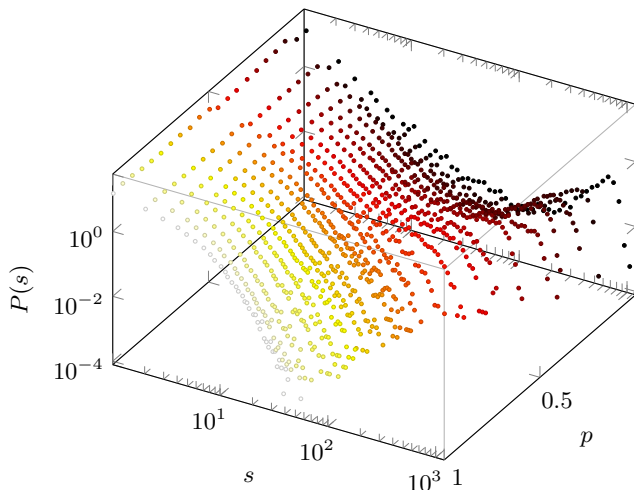


FIG. 3. Avalanche size distributions for different rewiring probabilities p . As connections become delocalised, the system shifts from supercritical to subcritical. The p -axis is reversed for visualisation purposes.

For low values of p , when connections are highly localised, the system is supercritical – the avalanche size distribution is characterised by a prominent peak at the far tail, which indicates that a disproportionately large fraction of the avalanches are strongly energetic and saturate the modules.

Conversely, at high values of p the system is subcritical. Avalanches are weak and the avalanche size distribution has a short exponential tail. This is probably caused by the diffuseness of the connectivity pattern – rewiring keeps the global synaptic strength fixed, but the influence of each burst of activity is spread across the whole network instead of focalised in one single module.

It is at middle that the activity of the modules resembles the activity of a critical system. Avalanche size distributions show power law-like statistics, with a characteristic

straight line in the log-log histogram and a small protuberance at the end, result of finite-size effects. To test the claim that the behaviour of the system is closest to a power law at an intermediate value of p , we perform a maximum-likelihood power law fit to each trial and calculate the 1-sample Kolmogorov-Smirnov (KS) statistic between the measured data and the fitted power law. The results, together with three representative histograms are shown in Fig. 4.

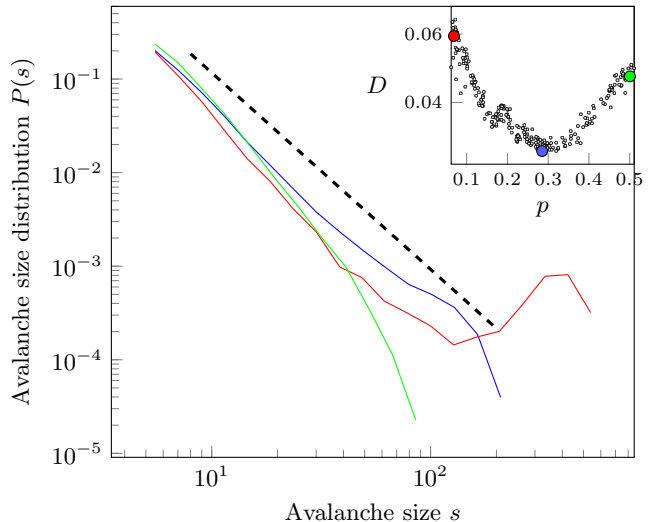


FIG. 4. Avalanche size distributions for three runs of the simulation, supercritical (red), subcritical (green) and critical (blue). Black line: reference $\alpha = -2$ power law as reported by [6, Fig. 3A] for 1 ms-binned LFP data. Inset: Kolmogorov-Smirnov statistic D comparing the data against a theoretical power law with the estimated parameters. Filled circles in the inset correspond to the runs shown in the main plot.

This figure more clearly shows the difference between critical, subcritical and supercritical behaviour; and the KS statistic determines that at $p = 0.3$ the system's avalanche size distribution is closest to a power law. Furthermore, at that point the critical exponent of the maximum-likelihood fit is consistent with the $\alpha \approx -2$ value found by Beggs and Plenz for 1 ms-binned LFP data and by de Arcangelis and Herrmann in simulations of realistic scale-free network topologies [6, 12].

C. Information-theoretic analysis

In practice, the challenge behind computing information-theoretic measures amounts to estimating probability densities for the involved quantities (e.g. $p(S_t)$ and $p(M_{i,t})$ in the case of TI). For our analyses we use the nearest-neighbour estimators devised by Kraskov, Stögbauer and Grassberger [17]. The KSG estimators are non-parametric and make only weak assumptions on the local neighbourhoods of the estimated probability density, which makes

them a robust, flexible tool. Reported results are corrected with surrogate data methods [25].

First, we show in Fig. 5 the total information TI between all 8 modules of the network. As p becomes large, the modules blend together and the system's TI increases, reflecting the increase in instantaneous correlation and synchronisation between the modules. This is evidence for cooperation between the modules in the high- p regime. Conversely, for $p = 0$ the modules are disconnected and TI is much lower. Note, however, that the modules have information about each other because they still interact indirectly through the inhibitory pool.

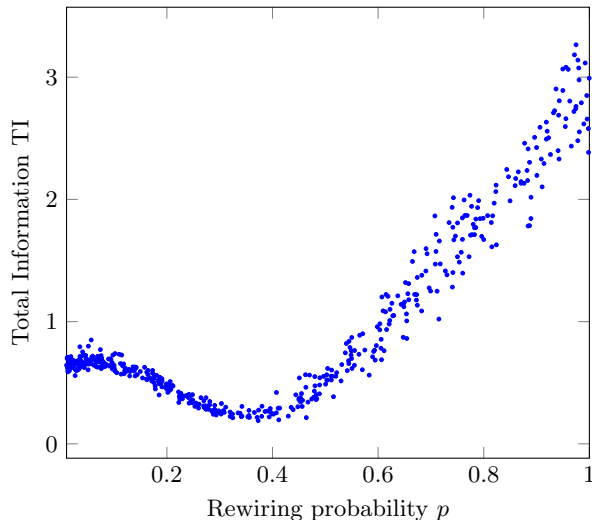


FIG. 5. Total Information (TI) between all 8 excitatory modules in the network. TI is maximal in the high- p regime, when modules are indistinguishable. In the middle, where the topology of the network is more complex, TI drops as the dynamics become more chaotic.

More importantly, we measure information storage and transfer with AIS and CD and show the results in Fig. 6. AIS is calculated separately for each module and then the 8 modules are averaged for each run. Nonparametric CD is calculated as described in section II A. The embedding dimension k is fixed at 5 for all calculations.

First we note that information storage dominates the low- p regime. Because of the WTA competition mechanism, if a module is inactive it tends to remain inactive, whereas if it is active it will most likely saturate and cease activity shortly after. This means that the recent history of the module's activity is highly informative of their future.

Regarding transfer, CD has a prominent peak in the mid- p region. As expected, there is little transfer in the $p = 0$ or $p = 1$ extremes, away of the neighbourhood around the critical transition. This is because in the low- p regime the modules are completely disconnected; and in the high- p regime the modules are so correlated that module i no longer provides information about j after conditioning on $S^{[i,j]}$.

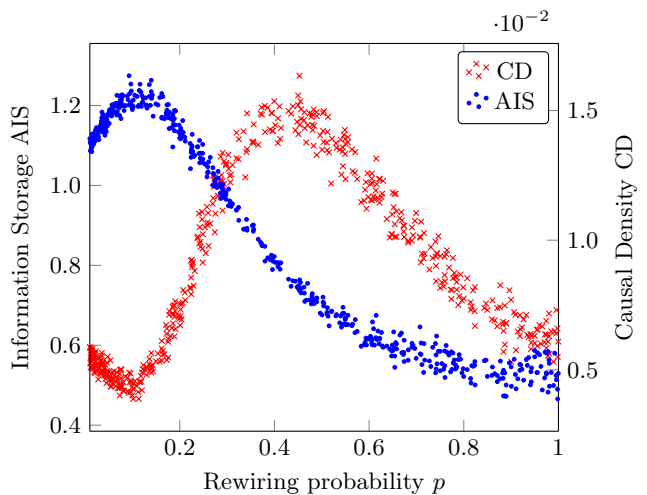


FIG. 6. Active information storage (blue, left axis) and non-parametric causal density (red, right axis) for different rewiring probabilities p . Each measure peaks at one side of the critical region around $p = 0.3$ where the system shows power law-like statistics (see Fig. 4).

More interesting is the neighbourhood around $p = 0.3$, where storage and transfer are maximally balanced. This coincides with the point where the avalanche dynamics are closest to a power law, as measured by the KS statistic and shown in Fig. 4. This suggests that there is a configuration of the system in which the balance between local and global coupling results in a balance between local information storage and long-range information transfer, which moreover is accompanied by a near-critical avalanche distribution. This finding links together three complementary views on neural computation: topological, informational and dynamical complexity.

D. Criticality and linear interactions

As we have argued above, the system exhibits a transition from competitive to cooperative dynamics as coupling shifts from short- to long-range. This transition is accompanied, in the large scale, by power law-like avalanche statistics. In this section we explore the signatures of such transition in the pairwise interactions between modules in different frequency bands.

To study the spectral aspects of the interaction, we analyse the data under three filtering conditions:

D0: Unfiltered data.

D1: After first-order differencing ($X'_t = X_t - X_{t-1}$).

D2: After second-order differencing ($X''_t = X'_t - X'_{t-1}$).

Since time-differencing is essentially a highpass filter, by taking successive differences we are effectively exploring higher regions of the network's frequency spectrum.

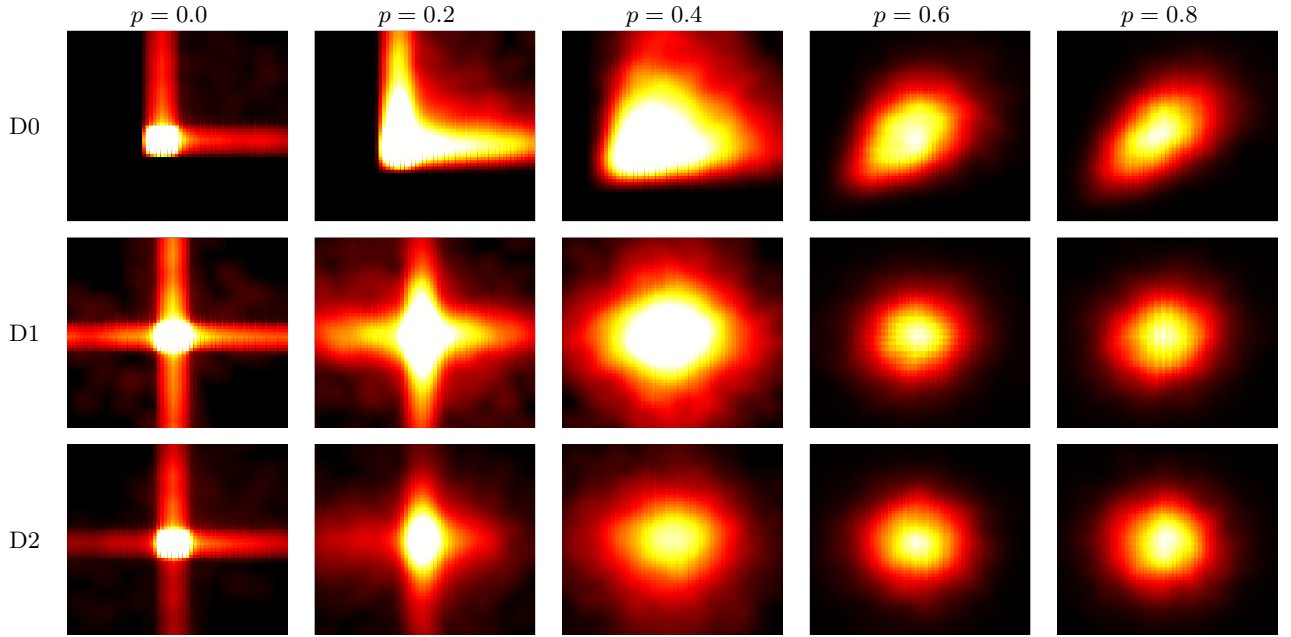


FIG. 7. Smoothed histograms of pairwise module interactions. As the rewiring probability p increases, interactions shift from nonlinear to linear. Time differencing acts as a highpass filter that adds stationarity to the data, but also affects the information content of the signal. Histograms are centered at the mean of each distribution and are 3σ wide.

Figure 7 shows aggregated histograms of the activity of all pairs of modules for growing values of p and the three filtering conditions.

For high p the pairwise interactions visually appear Gaussian, suggesting that interactions are mostly linear in this regime. For lower p , however, the WTA dynamics are clearly visible and interaction is heavily nonlinear. Interestingly, the transition between linear and nonlinear interaction lies in the $p \in (0.2, 0.4)$ range, where information processing is most diverse and avalanches exhibit power law-like statistics.

As a rough quantitative measure for nonlinearity, we calculate how much information is accounted for by linear interactions. To do so we compare MI between modules using two methods: the nonparametric KSG estimator, and a parametric estimator under the assumption that all interactions are linear with Gaussian noise.

The latter is referred to as the *linear-Gaussian* estimator, and it assumes that all variables in the system are jointly distributed as a multivariate Gaussian distribution. In this case all relevant information-theoretic quantities can be calculated analytically from the joint covariance matrix of the system [10, Chapter 9]. Under this assumption, the nonlinear component of the interaction is ignored.

To illustrate the effect of this assumption-breaking on informational measures, in Fig. 8 we show the average MI between all pairs of modules (i.e. the MI between the two variables shown in the histograms of Fig. 7) calculated with the linear-Gaussian estimator and with the nonparametric KSG estimator.

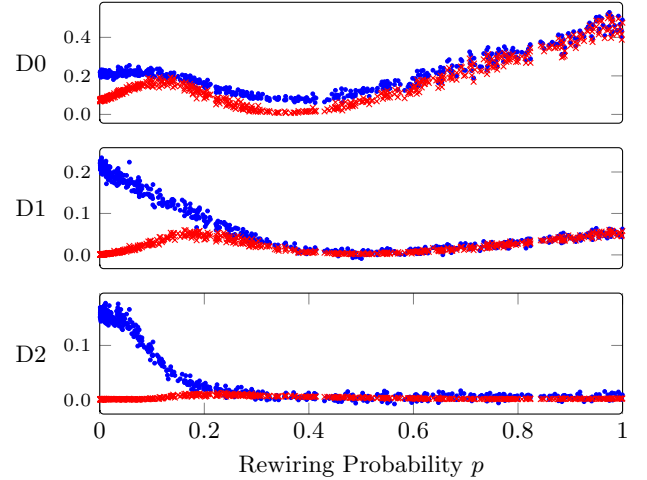


FIG. 8. MI between pairs of modules using linear-Gaussian (red) and nonparametric (blue) estimators.

As expected, the linear estimator always lies (up to random fluctuations) below the KSG. By considering linear interactions only and ignoring the rest, linear methods effectively provide a lower bound of the true MI. The linear-Gaussian estimator is close to the KSG for high p but consistently below it in the low- p range, which validates our claim that interactions shift from nonlinear to linear with increasing p . Furthermore, the gap between both estimators is more prominent in the differenced time series D1 and D2, indicating that the linear component of the interaction is carried by lower frequencies, which are more strongly suppressed by time-differencing.

IV. CONCLUSION

In this paper we studied a simple modular spiking neural network and used it to explore the relation between dynamics, information processing and underlying network topology. The fully modular setting implements a WTA mechanism, whereas the fully random setting is comparable to a PING oscillator – both of which are ubiquitous neural circuits in biological brains. This model gives us a way of interpolating between the two in a continuous fashion by varying a long-range connectivity parameter, p .

We find that for intermediate values of p the network passes through a near-critical regime in which avalanches

display power law-like statistics, with the same critical exponent as found in biological brains [6]. Measures of information storage and transfer peak at either side of the critical point, and the point where they are maximally balanced coincides with the point where avalanches are closest to a power law.

This transition can also be understood as a breakdown of linearity, with cooperative linear interaction being prevalent when connectivity is global and delocalised, and competitive winner-take-all interaction more prominent when connectivity is local.

Taken together, these findings link together three complementary views on neural computation: topological, informational, and dynamical complexity.

-
- [1] Alstott, J., Bullmore, E. T., and Plenz, D. (2013). Powerlaw: a Python Package for Analysis of Heavy-tailed Distributions.
 - [2] Balduzzi, D. and Tononi, G. (2008). Integrated Information in Discrete Dynamical Systems: Motivation and Theoretical Framework. *PLoS Computational Biology*, 4(6):e1000091.
 - [3] Barnett, L., Barrett, A. B., and Seth, A. K. (2009). Granger Causality and Transfer Entropy Are Equivalent for Gaussian Variables. *Physical Review Letters*, 103(23):238701.
 - [4] Barnett, L. and Bossomaier, T. (2012). Transfer Entropy as a Log-Likelihood Ratio. *Physical Review Letters*, 109(13):138105.
 - [5] Beer, R. D. and Williams, P. L. (2014). Information Processing and Dynamics in Minimally Cognitive Agents. *Cognitive Science*, 39(1):1–38.
 - [6] Beggs, J. M. and Plenz, D. (2003). Neuronal Avalanches in Neocortical Circuits. *The Journal of Neuroscience*, 23(35):11167–11177.
 - [7] Borst, A. and Theunissen, F. E. (1999). Information Theory and Neural Coding. *Nature Neuroscience*, 2(11):947–957.
 - [8] Buzsáki, G. and Wang, X.-J. (2012). Mechanisms of Gamma Oscillations. *Annual Review of Neuroscience*, 35(1):203–225.
 - [9] Clauset, A., Shalizi, C. R., and Newman, M. E. J. (2007). Power-law Distributions in Empirical Data.
 - [10] Cover, T. M. and Thomas, J. A. (2006). *Elements of Information Theory*. Wiley, Hoboken.
 - [11] Dayan, P. and Abbott, L. F. (2001). *Theoretical Neuroscience: Computational and Mathematical Modeling of Neural Systems*. MIT Press, Cambridge, MA.
 - [12] de Arcangelis, L. and Herrmann, H. J. (2010). Learning as a phenomenon occurring in a critical state. *Proceedings of the National Academy of Sciences*, 107(9):3977–81.
 - [13] Fidjeland, A. K., Roesch, E. B., Shanahan, M. P., and Luk, W. (2009). NeMo: A Platform for Neural Modelling of Spiking Neurons Using GPUs. In *2009 20th IEEE International Conference on Application-specific Systems, Architectures and Processors*, pages 137–144. IEEE.
 - [14] Hennequin, G., Gerstner, W., and Pfister, J.-P. (2010). STDP in Adaptive Neurons Gives Close-To-Optimal Information Transmission. *Frontiers in Computational Neuroscience*, 4:143.
 - [15] Izhikevich, E. M. (2003). Simple Model of Spiking Neurons. *IEEE Transactions on Neural Networks*, 14(6):1569–72.
 - [16] Johnson, D. H., Gruner, C. M., Baggerly, K., and Seshagiri, C. (2001). Information-Theoretic Analysis of Neural Coding. *Journal of Computational Neuroscience*, 10(1):47–69.
 - [17] Kraskov, A., Stögbauer, H., and Grassberger, P. (2004). Estimating Mutual Information. *Physical Review E*, 69(6):066138.
 - [18] Lizier, J. T. (2010). *The Local Information Dynamics of Distributed Computation in Complex Systems*. Springer Theses. Springer Berlin Heidelberg, Berlin, Heidelberg.
 - [19] Lizier, J. T. (2014). JIDT: An Information-Theoretic Toolkit for Studying the Dynamics of Complex Systems. *Frontiers in Robotics and AI*, 1:37.
 - [20] Lizier, J. T., Pritam, S., and Prokopenko, M. (2011). Information Dynamics in Small-world Boolean Networks. *Artificial Life*, 17(4):293–314.
 - [21] Lizier, J. T. and Prokopenko, M. (2010). Differentiating Information Transfer and Causal Effect. *European Physical Journal B*, 73:605–615.
 - [22] Lizier, J. T., Prokopenko, M., and Zomaya, A. Y. (2008). Local Information Transfer as a Spatiotemporal Filter for Complex Systems. *Physical Review E*, 77(2):026110.
 - [23] Lizier, J. T., Prokopenko, M., and Zomaya, A. Y. (2012). Local Measures of Information Storage in Complex Distributed Computation. *Information Sciences*, 208:39–54.
 - [24] Lochmann, T. and Denève, S. (2008). Information Transmission with Spiking Bayesian Neurons. *New Journal of Physics*, 10(5):055019.
 - [25] Lucio, J. H., Valdés, R., and Rodríguez, L. R. (2012). Improvements to Surrogate Data Methods for Nonstationary Time Series. *Physical Review E*, 85(5):056202.
 - [26] Mediano, P. A. M., Farah, J. C., and Shanahan, M. (2016). Integrated Information and Metastability in Systems of Coupled Oscillators.
 - [27] Priesemann, V., Wibral, M., Valderrama, M., Pröpper, R., Le Van Quyen, M., Geisel, T., Triesch, J., Nikolić, D., and Munk, M. H. J. (2014). Spike Avalanches in Vivo Suggest a Driven, Slightly Subcritical Brain State.

- Frontiers in Systems Neuroscience*, 8(108):108.
- [28] Prokopenko, M., Boschetti, F., and Ryan, A. J. (2009). An Information-theoretic Primer on Complexity, Self-organization, and Emergence. *Complexity*, 15(1):11–28.
 - [29] Pruessner, G. (2012). *Self-Organised Criticality: Theory, Models and Characterisation*. Cambridge University Press, Cambridge, UK.
 - [30] Schreiber, T. (2000). Measuring Information Transfer. *Physical Review Letters*, 85(2):461–464.
 - [31] Seth, A. K., Barrett, A. B., and Barnett, L. (2011). Causal Density and Integrated Information as Measures of Conscious Level. *Philosophical Transactions A: Mathematical, Physical and Engineering Sciences*, 369(1952):3748–67.
 - [32] Shanahan, M. (2008). Dynamical Complexity in Small-world Networks of Spiking Neurons. *Physical Review E*, 78(4):041924.
 - [33] Shew, W. L., Yang, H., Yu, S., Roy, R., and Plenz, D. (2011). Information Capacity and Transmission are Maximized in Balanced Cortical Networks with Neuronal Avalanches. *Journal of Neuroscience*, 31(1):55–63.
 - [34] Studený, M. and Vejnarová, J. (1999). The Multiinformation Function as a Tool for Measuring Stochastic Dependence. In Jordan, M., editor, *Learning in Graphical Models*, pages 261–297. MIT Press, Cambridge, US.
 - [35] Takens, F. (1981). Detecting Strange Attractors in Turbulence. In Rand, D. and Young, L.-S., editors, *Dynamical Systems and Turbulence*, pages 366–381. Springer Berlin Heidelberg, Berlin, Heidelberg.
 - [36] Tononi, G., Edelman, G. M., and Sporns, O. (1998). Complexity and Coherency: Integrating Information in the Brain. *Trends in Cognitive Sciences*, 2(12):474–484.
 - [37] Watts, D. J. and Strogatz, S. H. (1998). Collective Dynamics of ‘Small-world’ Networks. *Nature*, 393(6684):440–442.
 - [38] Wibral, M., Lizier, J. T., Vögler, S., Priesemann, V., and Galuske, R. (2014). Local Active Information Storage as a Tool to Understand Distributed Neural Information Processing. *Frontiers in Neuroinformatics*, 8:1.